Molecular Therapy
Nucleic Acids
Original Article

Long non-coding RNA *Mir22hg*-derived miR-22-3p promotes skeletal muscle differentiation and regeneration by inhibiting HDAC4

Rongyang Li,[1] Bojiang Li,[2] Yan Cao,[1] Weijian Li,[1] Weilong Dai,[1] Liangliang Zhang,[1] Xuan Zhang,[1] Caibo Ning,[1] Hongqiang Li,[1] Yilong Yao,[3] Jingli Tao,[1] Chao Jia,[1] Wangjun Wu,[1] and Honglin Liu[1]

[1]Department of Animal Genetics, Breeding and Reproduction, College of Animal Science and Technology, Nanjing Agricultural University, Nanjing 210095, China; [2]College of Animal Science and Veterinary Medicine, Shenyang Agricultural University, Shenyang 110866, China; [3]Genome Analysis Laboratory of the Ministry of Agriculture, Agricultural Genome Institute at Shenzhen, Chinese Academy of Agricultural Sciences, Shenzhen 518120, China

Emerging studies have indicated that long non-coding RNAs (lncRNAs) play important roles in skeletal muscle growth and development. Nevertheless, it remains challenging to understand the function and regulatory mechanisms of these lncRNAs in muscle biology and associated diseases. Here, we identify a novel lncRNA, *Mir22hg*, that is significantly upregulated during myoblast differentiation and is highly expressed in skeletal muscle. We validated that *Mir22hg* promotes myoblast differentiation *in vitro*. Mechanistically, *Mir22hg* gives rise to mature microRNA (miR)-22-3p, which inhibits its target gene, histone deacetylase 4 (*HDAC4*), thereby increasing the downstream myocyte enhancer factor 2C (*MEF2C*) and ultimately promoting myoblast differentiation. Furthermore, *in vivo*, we documented that *Mir22hg* knockdown delays repair and regeneration following skeletal muscle injury and further causes a significant decrease in weight following repair of an injured *tibialis anterior* muscle. Additionally, *Mir22hg* gives rise to miR-22-3p to restrict *HDAC4* expression, thereby promoting the differentiation and regeneration of skeletal muscle. Given the conservation of *Mir22hg* between mice and humans, *Mir22hg* might constitute a promising new therapeutic target for skeletal muscle injury, skeletal muscle atrophy, as well as other skeletal muscle diseases.

INTRODUCTION

Skeletal muscle is a highly dynamic and adaptive tissue that plays a pivotal role in regulating whole-body metabolism. However, disorders of skeletal muscle growth and development can lead to numerous diseases, such as muscular atrophy, dystrophy, hypertrophy, and myosarcoma.[1] Thus, identification of the functional components in muscle biology, as well as elucidation of their regulatory mechanisms, will aid toward identifying potential therapeutic approaches for muscular diseases.

Long non-coding RNAs (lncRNAs), a type of non-coding RNA comprised of >200 nucleotides, are involved in diverse biological processes throughout an organism's life span, including immunobiology,[2] cell fate,[3] cell differentiation and development,[4] and diseases.[5] lncRNAs act as regulators through multiple mechanisms, including chromosome modification, transcriptional activation, molecular sponge activity, competitive binding, mRNA translation, and protein stability.[6] In particular, numerous studies indicate that lncRNAs play an important role in skeletal muscle biology and muscular diseases,[7] as summarized in several reviews.[8,9] For example, linc-MD1, the first lncRNA identified as specifically expressed in muscle tissue, reportedly controls the differentiation of muscle cells by interacting with microRNA (miR)-133 and miR-135 as a molecular sponge and is related to muscle atrophy.[10] In addition, lnc-mg is highly expressed in skeletal muscle and is associated with muscle hypertrophy. It also serves as a competing endogenous RNA (ceRNA) against miR-125 to modulate insulin-like growth factor 2 (IGF2) levels, thereby regulating skeletal muscle differentiation.[11]

Currently, thousands of lncRNAs have been identified in skeletal muscles, and various skeletal muscle highly expressed lncRNAs and diverse regulatory mechanisms have been revealed.[12,13] Further, the roles and regulatory mechanisms of some classically defined lncRNAs have also been verified.[14,15] Nevertheless, it remains a tremendous challenge to understand the role of these molecules in the molecular mechanism in myogenesis and skeletal muscle growth as well as the development and molecular mechanisms of the thousands of lncRNAs that have been recently identified in skeletal muscles. Moreover, considering that skeletal muscle disease-related lncRNAs have been described, lncRNAs may represent a new potential therapeutic target for skeletal muscle diseases.[7,16]

Received 8 December 2020; accepted 22 February 2021;
https://doi.org/10.1016/j.omtn.2021.02.025.

Correspondence: Honglin Liu, Department of Animal Genetics, Breeding and Reproduction, College of Animal Science and Technology, Nanjing Agricultural University, Nanjing 210095, China.
E-mail: liuhonglin@njau.edu.cn
Correspondence: Wangjun Wu, Department of Animal Genetics, Breeding and Reproduction, College of Animal Science and Technology, Nanjing Agricultural University, Nanjing 210095, China.
E-mail: wuwangjun2012@njau.edu.cn

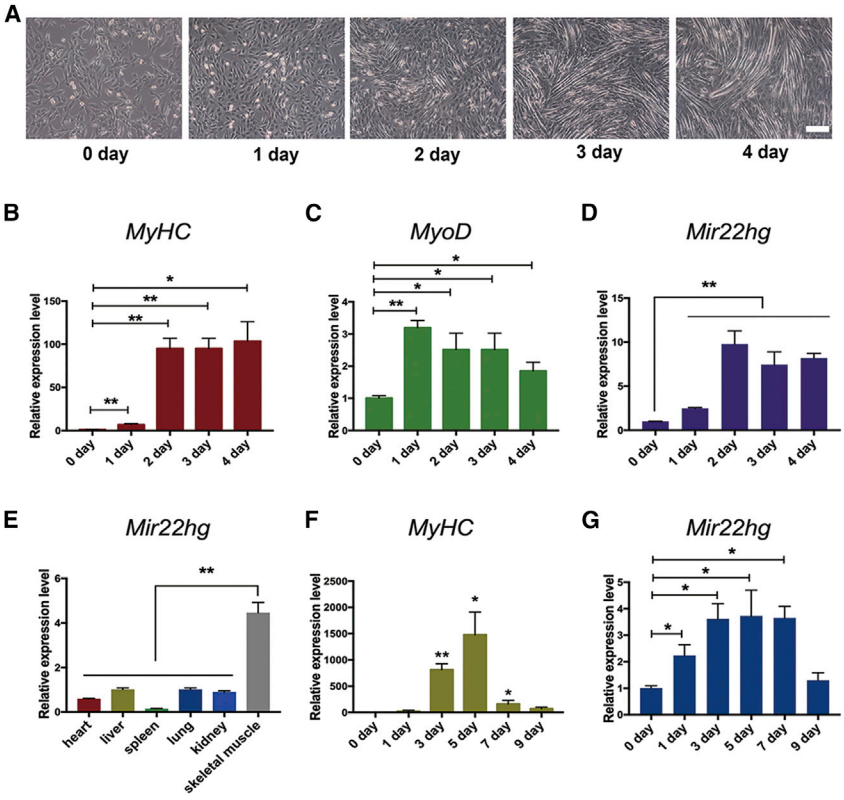

Figure 1. Expression patterns of lncRNA *Mir22hg*

(A) Morphology of differentiated C2C12 cells (n = 3). C2C12 myoblasts were induced to differentiate for 1, 2, 3, and 4 days in DM, and scale bars correspond to 100 μm. (B–D) qRT-PCR analysis of mRNA expression of *MyHC* (B), *MyoD* (C), and *Mir22hg* (D) in differentiated C2C12 cells (n = 3). (E) qRT-PCR analysis of *Mir22hg* expression in six different tissues of mice (n = 3). (F and G) qRT-PCR analysis of *MyHC* (F) and *Mir22hg* (G) mRNA expression in the process of skeletal muscle injury and repair (n = 3). Mouse *GAPDH* was used to normalize the gene expression levels as an endogenous reference gene during C2C12 differentiation, and mouse *HPRT* was used for tissue expression profile. Data are expressed as mean values ± SEM, and an unpaired two-tailed Student's t test was used to analyze the statistical significance between two groups. *p < 0.05, **p < 0.01.

In this study, we identified a new lncRNA, *Mir22hg*, that is characterized by high expression in skeletal muscle, for which we systematically defined its function in differentiation, repair, and regeneration. Our data indicated that *Mir22hg* promotes the differentiation of skeletal muscle cells *in vitro* and facilitates the repair and regeneration of injured skeletal muscle mass *in vivo*. Mechanistically, *Mir22hg* gives rise to miR-22-3p to inhibit the target gene histone deacetylase 4 (*HDAC4*), thereby promoting myocyte enhancer factor 2C (*MEF2C*) expression, myoblast differentiation, and the repair and regeneration of injured skeletal muscle.

RESULTS

Mir22hg expression patterns

By integrating previously published data, we revealed that 74 overlapping lncRNAs were annotated in the UCSC database as showing upregulation with the progression of myogenesis (Figure S1). Notably, some of the upregulated lncRNAs have been reported to play important roles in skeletal myogenesis, such as *H19*[17] and *2310043L19Rik*.[12,18] Moreover, in the study by Zhou et al.,[19] Gene Ontology (GO) function analysis showed that *Mir22hg* is involved in NADH oxidation in myoblasts and muscle contraction in myotubes (Figure S1); however, its function in skeletal myogenesis remained unclear.

Based on these results, we hypothesized that *Mir22hg* plays a crucial role in the differentiation of skeletal muscle cells. After 4 days of C2C12 differentiation, obviously fused myotubes were visible (Figure 1A), and the expression of differentiation markers *myosin heavy chain* (*MyHC*) (Figure 1B) and *MyoD* (Figure 1C) gradually increased during myogenesis. Consistent with our hypothesis, *Mir22hg* was also upregulated with increasing days of differentiation (Figure 1D), the trend for which was consistent with that of *MyHC* and *MyoD*, further confirming the previous RNA sequencing (RNA-seq) results.[19] In addition, tissue expression profile showed that *Mir22hg* was highly expressed in skeletal muscle (Figure 1E). Furthermore, in the process of regeneration following skeletal muscle injury, *MyHC* expression first increased and subsequently decreased (Figure 1F). Notably, *Mir22hg* also displayed a similar expression pattern (Figure 1G), suggesting that *Mir22hg* might play an important role in the process of myogenesis and skeletal muscle regeneration.

Mir22hg promotes myoblast differentiation

To explore its functional roles, we constructed a vector that efficiently overexpressed *Mir22hg* (Figure 2A) and detected the effect of *Mir22hg* on the differentiation of skeletal muscle cells. Immunofluorescence revealed that *Mir22hg* overexpression induced differentiation on the third day, concomitant with significant increases in the number of MyHC (Figures 2B and 2C)- and MyoG (Figures 2E and 2F)-positive cells, indicating that overexpression of *Mir22hg* promoted the formation of myotubes. Western blotting results confirmed that *Mir22hg* overexpression promoted the expression of MyHC protein (Figure 2D).

Moreover, we designed three short interfering (si)RNAs targeting *Mir22hg* and selected the one exhibiting the highest knockdown efficiency, siMir22hg-2, for subsequent experiments (Figure 2G). Conversely, the results showed that *Mir22hg* knockdown inhibited the expression of *MyoD* (Figure 2H) and *MyHC* (Figure 2I) at the mRNA level. Immunofluorescence results further demonstrated that knockdown of *Mir22hg* reduced MyHC expression (Figures 2J

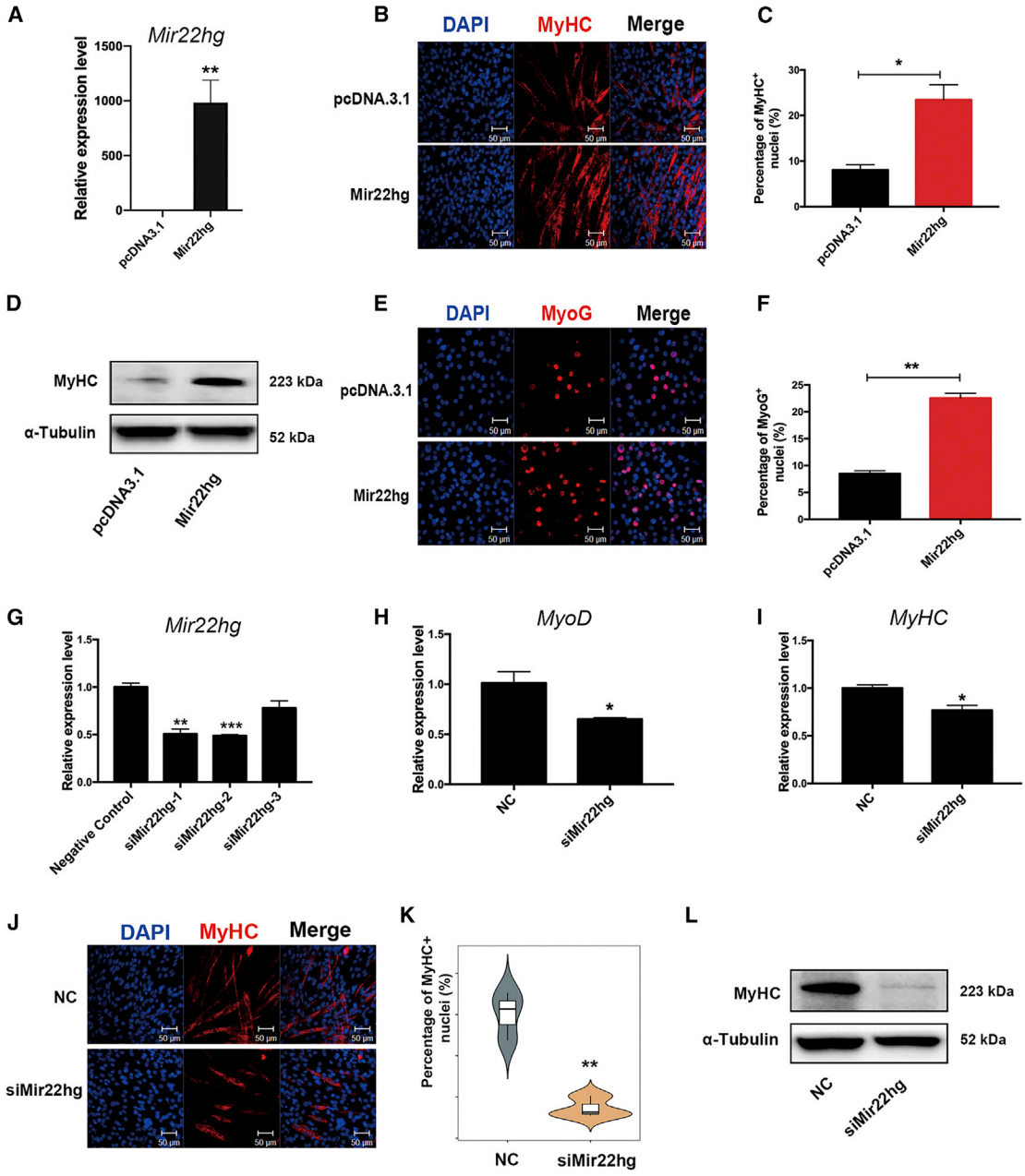

Figure 2. lncRNA *Mir22hg* enhances myoblast differentiation *in vitro*

(A) qRT-PCR analysis of *Mir22hg* expression in C2C12 cells transfected with control pcDNA3.1 or *Mir22hg* after 24 h in DM (n = 3). (B) Representative photographs of MyHC immunofluorescence staining in C2C12 cells differentiated for 4 days after overexpression of *Mir22hg*. (C) Quantitation of the MyHC-positive cells (n = 3). (D) Western blotting of MyHC in C2C12 cells differentiated for 3 days after overexpression of *Mir22hg*. (E) Representative photographs of MyoG immunofluorescence staining in C2C12 cells differentiated for 4 days after overexpression of *Mir22hg*. (F) Quantitation of the MyoG-positive cells (n = 3). (G) qRT-PCR analysis of *Mir22hg* knockdown in C2C12 cells transfected with control NC or three si*Mir22hg*s after 24 h (n = 3). (H and I) qRT-PCR analysis of mRNA expression of *MyoD* (H) and *MyHC* (I) in C2C12 cells transfected with negative control (NC) or si*Mir22hg* and then cultured in DM for 2 days (n = 3). (J) Representative photographs of MyHC immunofluorescence staining in C2C12 cells differentiated for 4 days after transfection with control NC or si*Mir22hg*. (K) Quantitation of the MyHC-positive cells (n = 3). (L) Western blotting of MyHC in C2C12 cells differentiated for 3 days after transfection with control NC or si*Mir22hg*. Data are expressed as mean values ± SEM, and an unpaired two-tailed Student's t test was used to analyze the statistical significance between two groups. *$p < 0.05$, **$p < 0.01$, ***$p < 0.001$.

and 2K), indicating that knockdown of *Mir22hg* inhibits the formation of myotubes. In addition, western blotting results revealed that *Mir22hg* knockdown significantly decreased MyHC protein levels (Figure 2L). Hence, *Mir22hg* serves as a critical positive regulator of myoblast differentiation.

Mir22hg promotes myoblast differentiation via miR-22-3p

To understand the role of *Mir22hg* in skeletal muscle cell differentiation, we performed bioinformatics analysis and found that *Mir22hg* was also highly conserved across many species, including humans and mice in addition to livestock animals (Figure S2), with the miR-22-3p-containing region of *Mir22hg* particularly highly conserved (Figure S3A). These results suggested that *Mir22hg* may exert its function by producing the conserved miR-22-3p. Furthermore, quantitative reverse transcription polymerase chain reaction (qRT-PCR) results showed that miR-22-3p levels gradually increased during differentiation (Figure S3B), and its expression was significantly positively correlated (r = 0.732, p = 0.0019) with that of *Mir22hg* during differentiation (Figure S3C). In turn, tissue expression profile indicated that miR-22-3p was also highly expressed in skeletal muscle and myocardium (Figure S3D), and its expression was significantly increased in C2C12 cells overexpressing *Mir22hg* (Figure S3E). Accordingly, we deduced that mature miR-22-3p might be derived from *Mir22hg*. To confirm this hypothesis, we investigated the effects of mutating the miR-22-3p seed sequence in the *Mir22hg* sequence on the expression of mature miR-22-3p. qRT-PCR results showed that miR-22-3p expression in the *Mir22hg*-mut group was significantly lower than that in the *Mir22hg* group, whereas no difference was observed compared with the control group (Figure S3F). Together, these results demonstrated that *Mir22hg* could yield mature miR-22-3p after shearing through post-transcriptional processing.

HDAC4, a direct target of miR-22-3p, is crucial for the function of *Mir22hg*

To explore the regulatory mechanism of *Mir22hg*, we first examined the cytoplasmic and nuclear distribution of *Mir22hg* in C2C12 cells. The results of the nucleocytoplasmic separation assay and RNA fluorescence *in situ* hybridization (RNA-FISH) showed that *Mir22hg* was highly expressed in the cytoplasm (Figures 3A and 3B). As *Mir22hg* produced miR-22-3p through processing in C2C12 cells, we proposed that *Mir22hg* might function by modulating miR-22-3p targets. Accordingly, we predicted the target genes of miR-22-3p, using three online tools: miRTarBase, TargetScan, and RNA22. As shown in the Venn diagram, seven overlapping target genes were predicted, including *ERBB3*, *HDAC4*, *MECP2*, *DDIT4*, *KLF6*, *VSNL1*, and *SCAMP1*(Figure 3C). As *HDAC4* is reported to inhibit myogenic differentiation and to promote C2C12 cell proliferation,[20] we subsequently focused our attention on the *HDAC4* gene. To verify whether *HDAC4* was affected by miR-22-3p, we constructed wild-type (HDAC4-WT) and mutant (HDAC4-Mut) luciferase reporter vectors (Figure 3D) and performed dual-luciferase reporter assays. Results showed that the relative luciferase activity was significantly decreased after co-transfection of HDAC4-WT and miR-22-3p in HEK293T cells (Figure 3E). Furthermore, immunofluorescence results revealed that overexpression of miR-22-3p significantly inhibited the expression of HDAC4 (Figures 3F and 3G). These findings were supported by the results of western blotting (Figure 3H).

To further confirm the inhibitory effect of *Mir22hg* on HDAC4 by generating miR-22-3p, we performed a co-transfection experiment. Immunofluorescence results showed that the expression of HDAC4 was significantly decreased in the miR-22-3p overexpression group (pcDNA3.1 + mimics miR-22-3p) compared with that in the control group (pcDNA3.1 + mimics negative control (NC); Figures 4A and 4B). Similarly, the expression of HDAC4 was significantly decreased in the *Mir22hg* overexpression group (Mir22hg + mimics NC) compared with that in the control group (pcDNA3.1 + mimics NC), whereas the expression level of HDAC4 could be rescued in *Mir22hg*-overexpressing cells through the addition of a miR-22-3p inhibitor (Figures 4A and 4B). Moreover, western blotting results demonstrated that co-transfection of *Mir22hg* and the miR-22-3p inhibitor rescued the expression of HDAC4 (Figure 4C). Collectively, these results indicated that *HDAC4* is a direct target of miR-22-3p and that *Mir22hg* inhibits HDAC4 expression through the generation of miR-22-3p.

HDAC4 is a negative regulator of myoblast differentiation

To confirm the role of *HDAC4* in myoblast differentiation, we designed three siRNAs and selected siRNA-3, which exhibited the highest knockdown efficiency, for subsequent experiments (Figure S4A). Knocking down HDAC4 significantly increased expression of the downstream transcription factor MEF2C, which is known to promote myoblast differentiation.[21] In addition, immunofluorescence results showed that knockdown of HDAC4 significantly increased the rate of MyHC (Figures S4B and S4C)- and MyoG (Figures S4D and S4E)-positive cells. These results indicated that HDAC4 serves as a negative regulator of myoblast differentiation.

Mir22hg targets HDAC4 through miR-22-3p to regulate myoblast differentiation

To demonstrate the promoting effect of *Mir22hg* on myoblast differentiation by generating miR-22-3p to inhibit *HDAC4* expression, we carried out a co-transfection experiment. Overexpression of miR-22-3p or *Mir22hg* promoted myotube formation (Figure 5A). Moreover, *Mir22hg* overexpression significantly increased the proportion of MyHC (Figures 5B and 5C)- and MyoG (Figures 5D and 5E)-positive cells. Compared with the group transfected with *Mir22hg* alone, the rate of MyHC- and MyoG-positive cells was significantly decreased in the group co-transfected with *Mir22hg* and the miR-22-3p inhibitor (Figures 5B–5E). Similarly, western blotting results revealed that transfection with *Mir22hg* or miR-22-3p increased MyHC and MyoG protein levels (Figure 5F) compared with those of the control group. Meanwhile, the protein levels of MyHC and MyoG significantly decreased in the group co-transfected with *Mir22hg* and miR-22-3p inhibitor compared with those in the group transfected with *Mir22hg* alone, which was consistent with the immunofluorescence results.

Furthermore, we induced mutations in the miR-22-3p seed sequence of *Mir22hg* and performed transfection experiments in C2C12 cells.

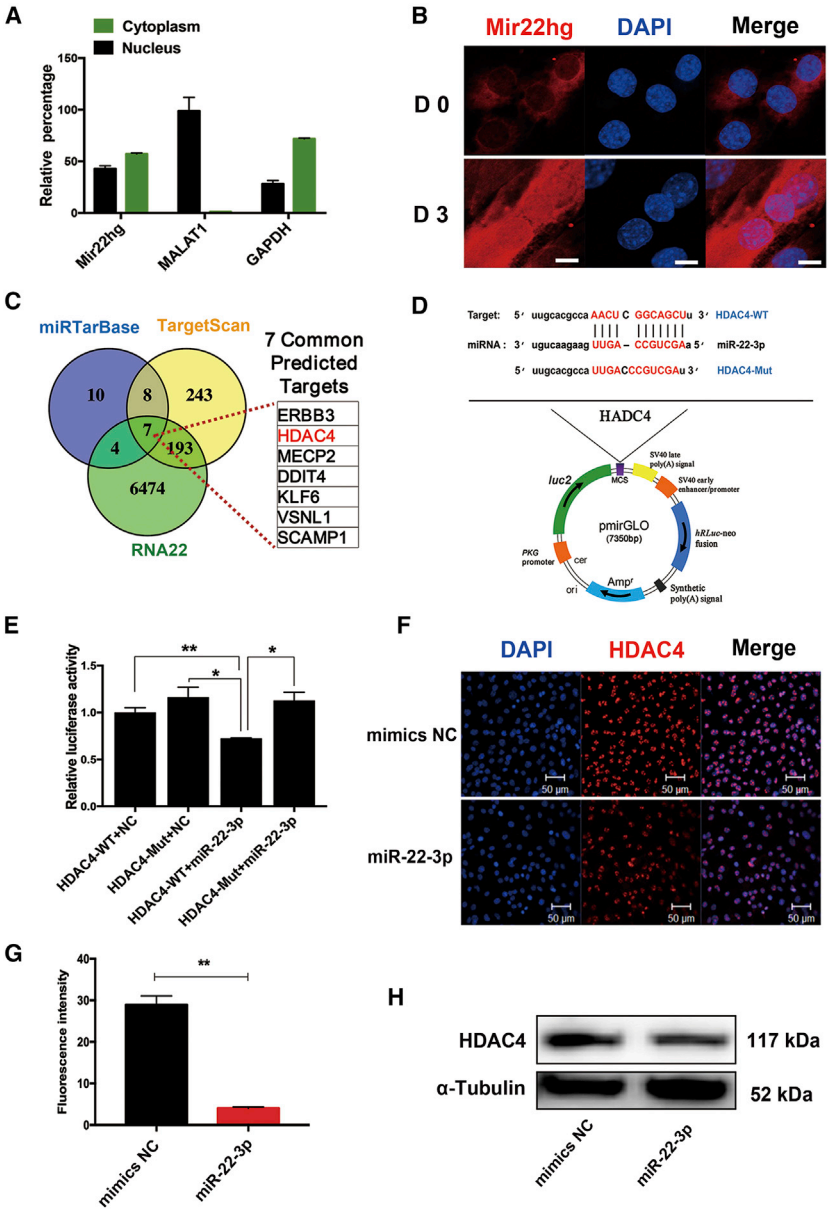

Figure 3. miR-22-3p directly targets *HDAC4*

(A) Nuclear-cytoplasmic separation test of *Mir22hg*, *MALAT1*, and *GAPDH* in C2C12 cells differentiated in DM for 2 days (n = 3). (B) RNA FISH showed localization of *Mir22hg* in the cell-proliferating C2C12 myoblasts (D0) and in C2C12 myoblasts differentiated for 3 days (D3), and scale bars correspond to 10 μm. (C) Venn diagram of overlapping target genes. The target genes were predicted with three bioinformatics software (miRTarBase, TargetScan, and RNA22). (D) Construction of vectors including wild-type (HDAC4-WT) and mutant (HDAC4-Mut) sequences of *HDAC4*. (E) Determination of luciferase activities. miR-22-3p mimics and NC mimics were co-transfected with the pmirGLO-HDAC4 luciferase vector (HDAC4-WT) or pmirGLO-HDCA4-Mut vector (HDAC4-Mut) into HEK293T cells for 24 h, and the normalized relative luciferase activities (*Renilla*/firefly) were determined (n = 3). (F) Immunofluorescence analysis of HDAC4 protein expression after transfection with miR-22-3p mimics and NC mimics. (G) Detection of fluorescence intensity of HDAC4 (n = 3). Fluorescence intensity was quantified with ImageJ. (H) Western blotting of HDAC4 protein expression after transfection of miR-22-3p mimics and NC mimics into C2C12 cells differentiated in DM for 2 days. Data are expressed as mean values ± SEM, and an unpaired two-tailed Student's t test was used to analyze the statistical significance between two groups. *$p < 0.05$, **$p < 0.01$.

Western blotting results showed that, compared with the *Mir22hg*-WT group, the *Mir22hg*-mut group exhibited significantly increased HDAC4 protein expression, while decreasing that of MEF2C (Figure S5A). In addition, *Mir22hg*-mut failed to promote the expression of MyHC (Figures S5B and S5C) or MyoG (Figures S5D and S5E). In summary, our data showed that *Mir22hg* regulated C2C12 differentiation by producing miR-22-3p to inhibit HDAC4.

Knockdown of *Mir22hg* delays regeneration following skeletal muscle injury

After skeletal muscle injury, quiescent skeletal muscle satellite cells are activated and migrate to the injury sites to rapidly proliferate and differentiate to participate in skeletal muscle repair and regeneration.[22] As our results confirmed that *Mir22hg* could promote myoblast differentiation, we speculated that *Mir22hg* might also be involved in the regeneration of injured skeletal muscle. To confirm this speculation, we generated a *Mir22hg*-knockdown short hairpin (sh)RNA lentivirus and performed a lentiviral injection experiment *in vivo*. The experimental design, including times of lentiviral and 1.2% $BaCl_2$ (causing muscle injury) injection and sample collection time, are shown in Figure 7A. After 2 days, the evaluation of *Mir22hg* knockdown efficiency in the TA muscles revealed that its expression was reduced by >60% (Figures 6B and 6C). Next, we carried out regeneration experiments after skeletal muscle injury. Hematoxylin and eosin (H&E) staining results showed that the rate of skeletal muscle repair was slower in the *Mir22hg* knockdown group compared with the control group (Figure 6D). Moreover, after 9 days, many of the nuclei remained in the center of the muscle fiber in the *Mir22hg* knockdown group, whereas in the control group most of the muscle fiber nuclei had migrated to the edge of muscle fibers, as is characteristic of mature fibers. These results indicated that *Mir22hg* knockdown inhibited the regeneration of injured skeletal muscle. In addition, in the *Mir22hg* knockdown group *tibialis anterior* (TA) muscle weight was significantly lower than that of the control group at day 12 (Figures 6E

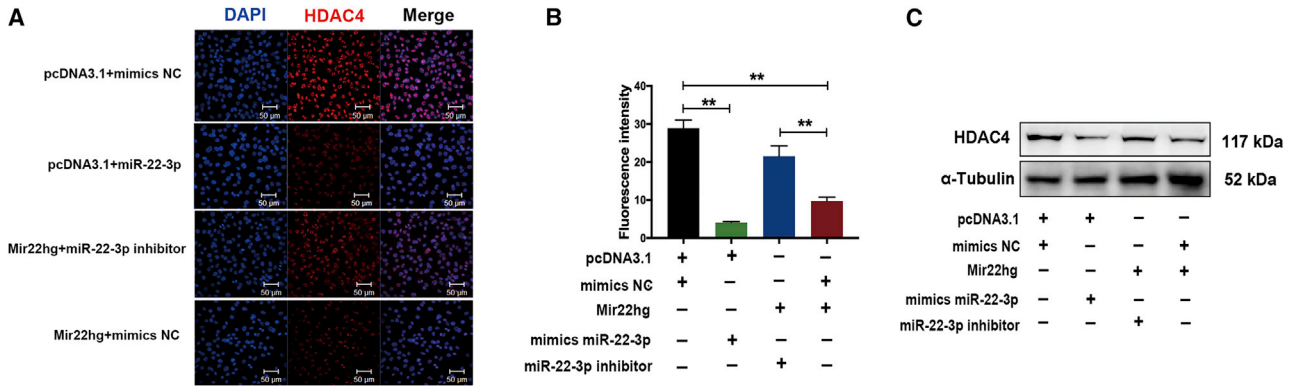

Figure 4. lncRNA *Mir22hg* regulates HDAC4 via miR-22-3p

(A) Immunofluorescence analysis of HDAC4 expression. C2C12 cells were co-transfected with pcDNA3.1 + mimics NC, pcDNA3.1 + mimics miR-22-3p, *Mir22hg* + miR-22-3p inhibitor, and *Mir22hg* + mimics NC, and the cells were cultured in DM for 2 days, after which immunofluorescence staining of HDAC4 was performed. (B) Detection of fluorescence intensity of HDAC4. Fluorescence intensity was quantified with ImageJ (n = 3). (C) Western blotting of HDAC4 protein expression in the same co-transfection assays. Data are expressed as mean values ± SEM, and an unpaired two-tailed Student's t test was used to analyze the statistical significance between two groups. **p < 0.01.

and 6F). Together, our data demonstrated that *Mir22hg* knockdown caused muscle weight loss consequent to the delayed regeneration of injured skeletal muscle.

Additionally, qRT-PCR results showed that the mRNA expression of *MyHC* and skeletal muscle α-actin was significantly lower in the *Mir22hg* knockdown group compared with the control group on days 1 and 3 during the repair process of injured TA muscle (Figures 7A and 7B). Similarly, MyHC and MyoG protein levels were significantly lower in the *Mir22hg* knockdown group than those in the control group on days 3, 5, 7, and 9 (Figure 7C). Conversely, HDAC4 protein in the *Mir22hg* knockdown group exhibited higher expression than that in the control group on days 7 and 9. In addition, we observed that *Mir22hg* expression was significantly positively correlated with the ratio of TA muscle to body weight ($r = 0.5055$, $p = 0.0084$; Figure 7D). Moreover, H&E staining results showed that the cross-sectional area of muscle fibers of the injured TA muscle was significantly lower in the *Mir22hg* group than in the control group (Figures 7E and 7F). These results indicated that *Mir22hg* knockdown in the TA muscle decreased the regenerative capacity of skeletal muscle fiber, thereby delaying the repair of injured muscle and ultimately leading to skeletal muscle weight loss and reduction of total skeletal muscle fiber area.

DISCUSSION

lncRNAs are characterized by fewer exons, are less evolutionarily conserved, and have lower expressed abundance but higher cell and tissue specificity than mRNA.[23,24] In this study, we screened *Mir22hg* as highly expressed in skeletal muscle based on previously published data sets[19,25] and demonstrated its ability to promote skeletal muscle differentiation and regeneration. Notably, the functional roles of *Mir22hg* were achieved through the generation of mature miR-22-3p to inhibit HDAC4, thereby enhancing the expression of MEF2C, a critical transcription factor for promoting myoblast differentiation.[26]

Among the diverse regulatory mechanisms, transcriptional activation and molecular sponges represent the most common regulatory mechanisms in skeletal myogenesis.[7] For example, some lncRNAs that are highly expressed in the cytoplasm primarily function as ceRNAs by acting as a molecular sponge to absorb miRNA, such as lnc-mg[11] and LncIRS1.[27] Other lncRNAs that are highly expressed in the nucleus, such as *SYISL*[25] and Linc-YY1,[28] execute their functions by interacting with transcription factors to activate or inhibit downstream target genes, thereby regulating the proliferation and differentiation of skeletal muscle. In the present study, we found that *Mir22hg* functions through the production of miR-22-3p, which then activates downstream pathways to promote skeletal muscle differentiation and regeneration. Indeed, a similar mechanism has been discovered in the skeletal muscle regulation of lncRNA *H19*, whose exon1 produces two conserved miRNAs, miR-675-3p and miR-675-5p.[17] We therefore further explored the precise regulatory mechanisms of *Mir22hg* in skeletal myogenesis.

We initially observed that the expression of *Mir22hg* was significantly increased during myoblast differentiation, whereas *Mir22hg* expression first increased and then decreased during the repair and regeneration of injured skeletal muscle, which is consistent with the change in MyHC expression in this process. These results suggest that *Mir22hg* may play an important role in regulating skeletal myogenesis *in vivo* and *in vitro*. Subsequently, we verified the functional roles of *Mir22hg* in promoting the differentiation of skeletal muscle cells through both overexpression and knockdown technologies. Notably, we observed that the mature miR-22-3p contained in the *Mir22hg* region is highly evolutionarily conserved across species. Moreover, miR-22-3p expression was markedly upregulated and significantly positively correlated with the expression of *Mir22hg* during myoblast differentiation and was also highly expressed in skeletal muscle. Our results further revealed that overexpression of *Mir22hg* significantly increased the expression of miR-22-3p, whereas mutating the seed

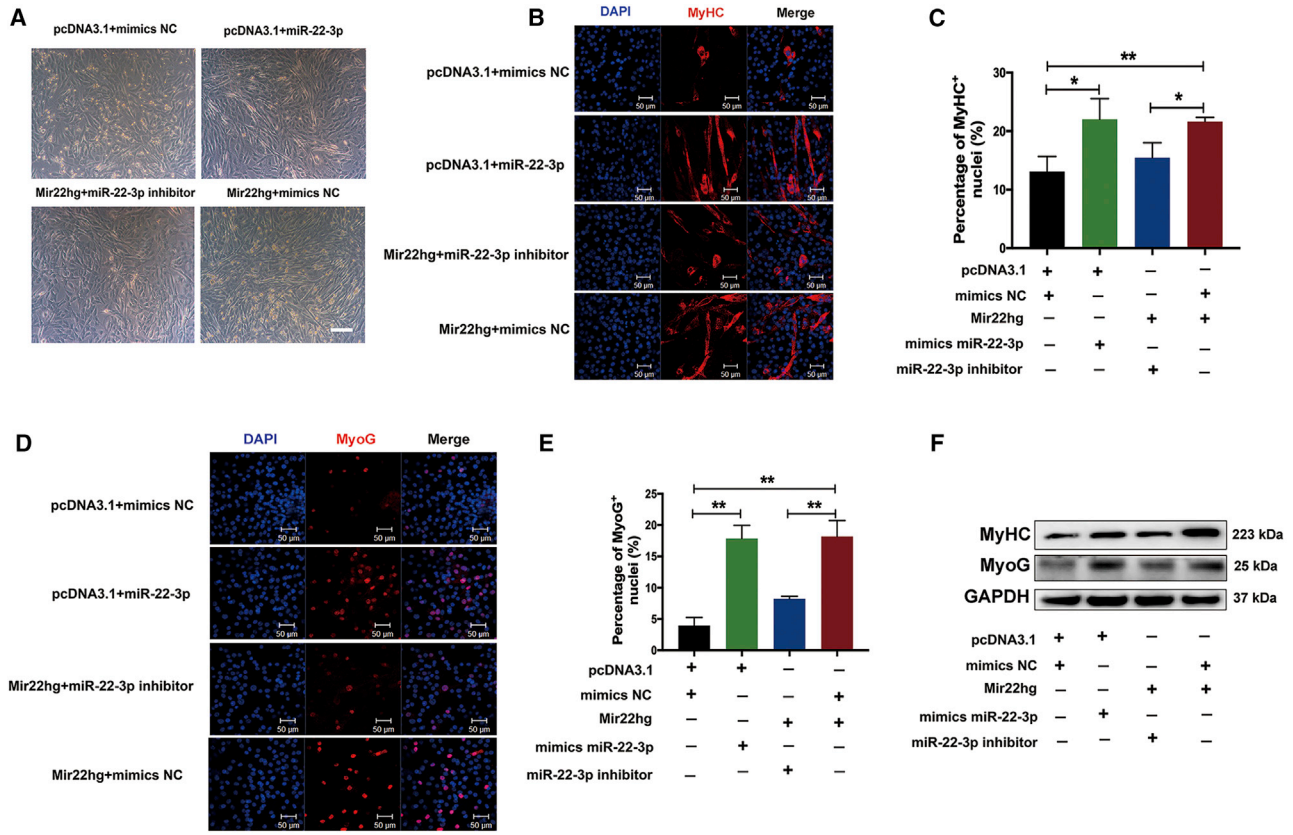

Figure 5. lncRNA *Mir22hg* regulates myoblast differentiation through miR-22-3p

(A) White light analysis of C2C12 differentiated 3 days after co-transfection. C2C12 were transfected with pcDNA3.1 + mimics NC, pcDNA3.1 + miR-22-3p, *Mir22hg* + miR-22-3p inhibitor, and *Mir22hg* + mimics NC; scale bars correspond to 100 μm. (B and D) Immunofluorescence analysis of MyHC (B) and MyoG (D) expression in different treatment groups. (C and E) Quantitation of MyHC (C) and MyoG (E) in different treatment groups (n = 3). (F) Western blotting of MyHC and MyoG protein expression after co-transfection in DM for 3 days. Data are expressed as mean values ± SEM, and an unpaired two-tailed Student's t test was used to analyze the statistical significance between two groups. *$p < 0.05$, **$p < 0.01$.

sequence of miR-22-3p in *Mir22hg* completely abolished miR-22-3p expression. Thus, these results indicate that *Mir22hg* executes its function of promoting skeletal muscle differentiation by generating mature miR-22-3p.

Subsequently, we predicted seven potential co-regulated target genes of miR-22-3p, using multiple bioinformatics tools. Among the encoded proteins, we focused our attention on HDAC4, a member of the HDAC family, because HDAC4 is critical for skeletal muscle differentiation and regeneration and regulates muscle-related diseases.[29,30] Next, we used a dual-luciferase reporter vector assay to demonstrate the targeting relationship between miR-22-3p and *HDAC4*. Moreover, overexpression of miR-22-3p or *Mir22hg* significantly inhibited the expression of HDAC4 *in vitro*. Further, knockdown of *HDAC4* promoted the differentiation of myoblasts by upregulating the expression of MEF2C, which is consistent with previous studies.[20,31] Conversely, myogenic differentiation was markedly inhibited when a miR-22-3p inhibitor was added to *Mir22hg*-overexpressing skeletal muscle cells. Recently, *lncMGPF* has been reported to regulate myogenesis by the MEF2C pathway.[32] Interestingly, *lncMGPF* also functions as a miRNA sponge of miR-135a-5p, weakening the inhibitory effects of miR-135a-5p on MEF2C and thereby increasing expression of the MEF2C. Both *lncMGPF* and *Mir22hg* are highly expressed in skeletal muscle and regulate myogenesis through the MEF2C pathway. Therefore, it will be interesting to explore the potential synergistic regulation of *lncMGPF* and *Mir22hg* in myogenesis in future study.

To further validate the function of *Mir22hg* during myogenesis, we constructed a murine skeletal muscle injury model and performed a lentiviral injection experiment to inhibit *Mir22hg* expression to observe the effect on injured skeletal muscle repair and regeneration. As expected, during the repair period following skeletal muscle injury, *Mir22hg* knockdown delayed skeletal muscle regeneration and significantly reduced TA muscle weight. Moreover, we observed that the gene expressions of differentiation-related factors (*MyHC*, *skeletal muscle α-Actin*) were significantly inhibited. In addition, the mean cross-sectional area of muscle fibers after regeneration was reduced

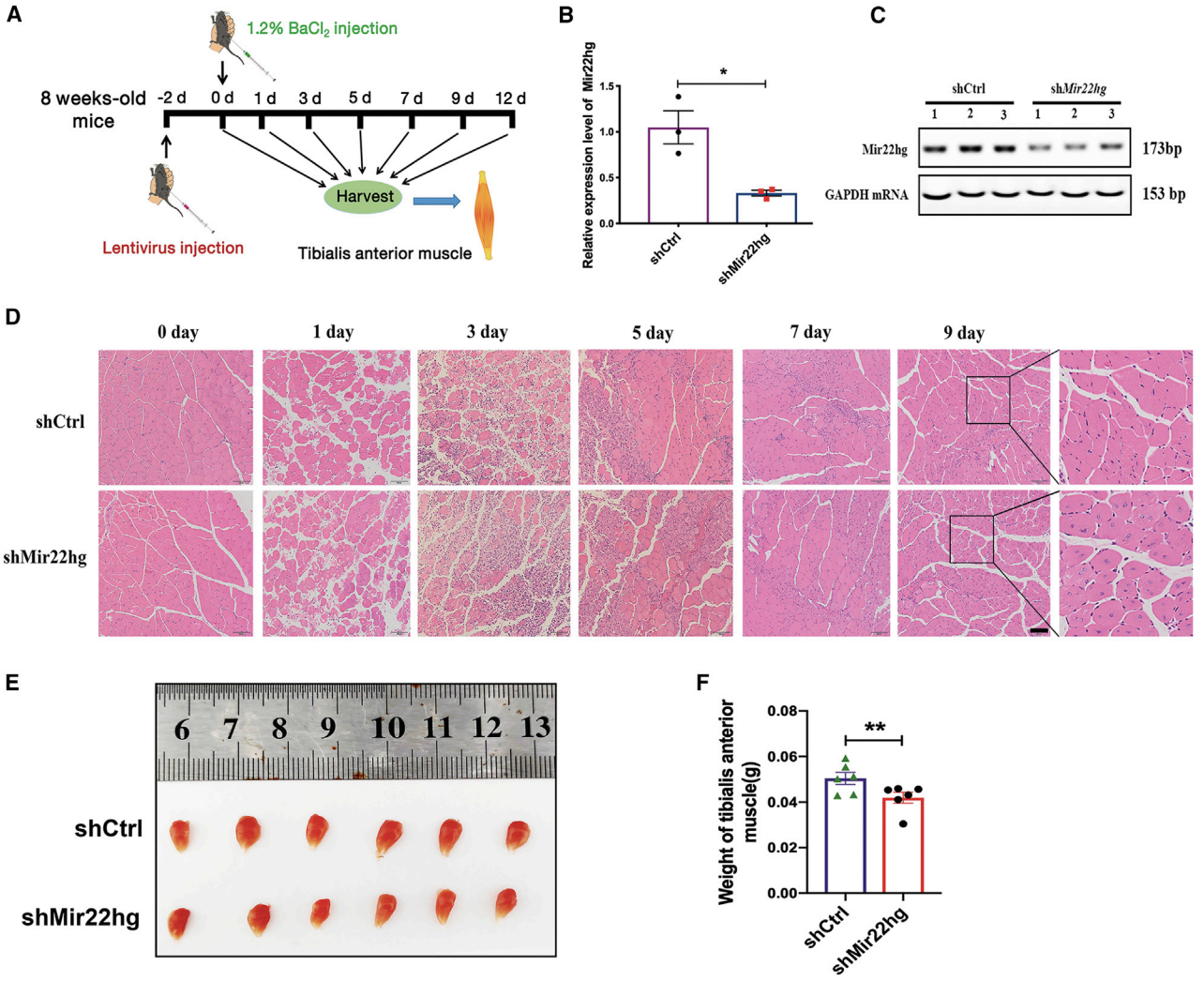

Figure 6. Lentiviral knockdown of lncRNA *Mir22hg* attenuates post-injury skeletal muscle regeneration

(A) Schematic diagram of lentivirus injection and muscle injury experiments. Control lentivirus was injected into the left leg of mice, and *Mir22hg* knockdown lentivirus was injected into the right leg. (B) qRT-PCR analysis of *Mir22hg* knockdown efficiency at 2 days of lentivirus injection (n = 3). (C) Semiquantitative RT-PCR analysis of *Mir22hg* knockdown efficiency (n = 3). (D) Comparison of H&E staining for the regeneration of TA muscle following injury. (E) Image of TA muscle injury at 12 days (n = 6). (F) Comparison of TA muscle weigh between the *Mir22hg* knockdown group and the control group. Data are expressed as mean values ± SEM, and a paired two-tailed Student's t test was used to analyze the statistical significance between two groups. *$p < 0.05$, **$p < 0.01$.

(Figure 8), and the expression of *Mir22hg* in the TA muscle was significantly positively correlated with the ratio of TA muscle to body weight. We speculated that satellite cell differentiation was partially inhibited after *Mir22hg* knockdown, leading to the slower formation of muscle fibers, thereby affecting regeneration after skeletal muscle injury. These results were similar to the regulatory mechanism by which lncRNAs H19 and MAR1 regulate skeletal muscle regeneration.[17,33] Therefore, our findings suggest that *Mir22hg* may constitute a new target for the treatment of skeletal muscle injury.

In summary, we identified a new lncRNA, *Mir22hg*, that is highly expressed in skeletal muscle and could give rise to mature miR-22-3p to inhibit HDAC4 expression, thereby activating the downstream MEF2C pathway to promote skeletal muscle differentiation and regeneration (Figure 8).[34,35] Our findings suggest that *Mir22hg* may be useful as a new therapeutic target for the treatment of skeletal muscle injury, skeletal muscle atrophy, and other muscular diseases.

MATERIALS AND METHODS

Pipeline for the discovery of candidate lncRNAs affecting skeletal muscle differentiation

To screen the critical candidate lncRNAs affecting skeletal muscle cell differentiation, we first downloaded lncRNA microarray data from various differentiation stages of mouse C2C12 from the study by

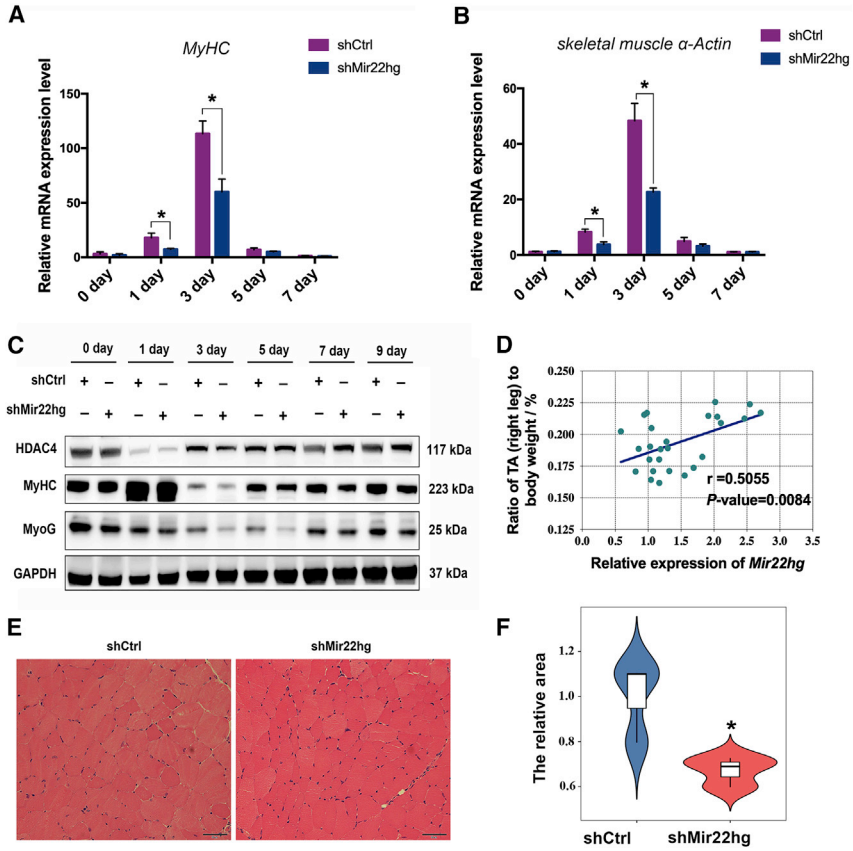

Figure 7. Knockdown of lncRNA *Mir22hg* decreases the expression of post-injury skeletal muscle regeneration-related genes

(A and B) qRT-PCR analysis of the mRNA expression level of (A) *MyHC* and (B) *skeletal muscle α-Actin* after *Mir22hg* knockdown in the TA muscle (n = 3). (C) Western blotting of HDAC4, MyHC, and MyoG protein expression after *Mir22hg* knockdown in the TA muscle. (D) Correlation analysis between the weight of TA muscle (right leg) and *Mir22hg* expression (n = 28). (E) H&E staining of the muscle fiber area of TA muscle. Control lentivirus was injected into the left leg of mice and *Mir22hg* knockdown lentivirus was injected into the right leg, and the regenerated TA muscles at 12 days after skeletal muscle injury were collected for H&E staining. (F) Quantitation of cross-sectional area of muscle fiber (n = 3). Quantification was conducted with ImageJ Pro Plus. Data are expressed as mean values ± SEM, and a paired two-tailed Student's t test was used to analyze the statistical significance between two groups. *$p < 0.05$.

Jin et al.[25] and conducted a comparative analysis with the lncRNAs identified in the C2C12 (mouse myoblast) differentiation process annotated in the UCSC database (https://genome.ucsc.edu/). Among the overlapping lncRNAs, 74 upregulated lncRNAs were annotated in the UCSC database. As the functions of one of these lncRNAs, *Mir22hg*, had also been predicted in myoblasts and myotubes in the study by Zhou et al.,[19] it was selected as a promising candidate lncRNA in skeletal myogenesis.

Animals

BALB/c mice were purchased from Qinglongshan Laboratory Animal Company (Nanjing, China). Mice were housed in specific pathogen-free rooms and kept under controlled conditions of temperature (20°C–23°C) and illumination (12 h light-dark cycle) and had free access to food and water throughout the study. All mice were handled following the Animal Research Institute Committee guidelines of Nanjing Agricultural University, China.

Cell culture and differentiation

Mouse C2C12 cells and human embryonic kidney HEK293T cells were cultured in high-glucose Dulbecco's modified Eagle's medium (DMEM; HyClone, Logan, UT, USA) supplemented with 10% (v/v) fetal bovine serum (Sigma-Aldrich, St. Louis, MO, USA) and 1% penicillin-streptomycin (Gibco, Grand Island, NY, USA) at a constant temperature of 37°C in 5% (v/v) CO_2. For the induction of C2C12 cell differentiation, C2C12 cells were induced with high-glucose DMEM supplemented with 2% horse serum and 1% penicillin-streptomycin.

Extraction of total RNA and qRT-PCR

Total RNA was extracted from mouse tissues and C2C12 cells with TRIzol reagent (Thermo Fisher Scientific, Waltham, MA, USA). The concentration and integrity of RNA were assessed with NanoDrop 2000 (Thermo Fisher Scientific). cDNA for mRNA and miRNA was synthesized with the PrimeScript RT Master Mix (Perfect Real Time, Takara) and Mix-X miRNA First-Strand Synthesis Kit (Takara), respectively. mRNA and miRNA detection was performed by qRT-PCR with AceQ qPCR SYBR Green Master Mix (Vazyme, Nanjing, China) on a Step-One Plus Real-Time PCR System (Applied Biosystems, Carlsbad, CA, USA). The primers for quantitative analyses are shown in Table S1. The relative expression levels were calculated with the $2^{-\Delta\Delta CT}$ method,[36] and mouse *GAPDH*, *U6* snRNA, and *Hprt* were used for normalization of gene expression levels as endogenous reference genes.

Cytoplasmic and nuclear lncRNA *Mir22hg*

Cytoplasmic and nuclear RNAs were extracted from C2C12 cells with protocols described previously.[37] In brief, the cells were washed with cold phosphate-buffered saline (PBS), lysed in cell lysis buffer from a Magna ChIP A/G Chromatin Immunoprecipitation Kit (Sigma-Aldrich), and centrifuged twice at 4°C. The supernatant was taken as the cytoplasmic fraction, and the bottom of the precipitate was collected as the nuclear fraction. RNA from the cytoplasmic and nuclear fractions were extracted with TRIzol reagent. The relative expression levels of *Mir22hg*, *Metastasis associated lung adenocarcinoma transcript 1* (*Malat1*), and *Gapdh* in both cytoplasmic and

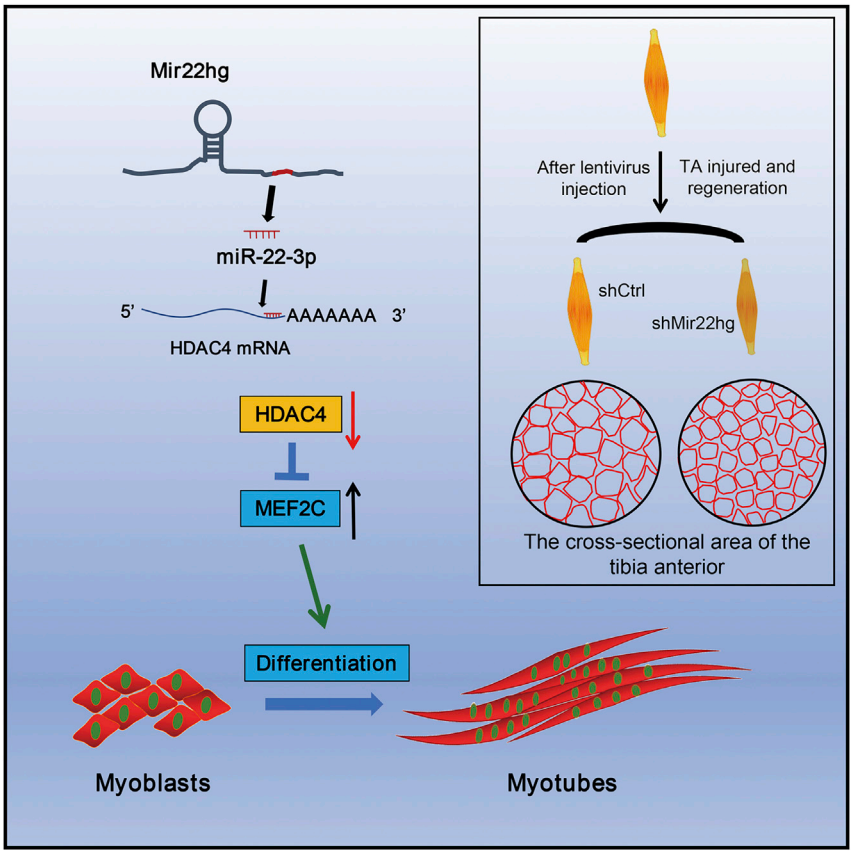

Figure 8. Molecular mechanism of lncRNA *Mir22hg*-mediated promotion of myoblast differentiation and regeneration

Injection of *Mir22hg* knockdown lentivirus into the TA muscle decreases the cross-sectional area of muscle fibers after repair of the injured muscle. lncRNA *Mir22hg* gives rise to mature miR-22-3p that inhibits expression of its target gene, *HDAC4*, thereby increasing downstream *MEF2C* expression and ultimately promoting the differentiation and regeneration of myoblasts.

nuclear fractions were determined by qRT-PCR. *Malat1*[38] was used as a reference for high expression of lncRNA in the nucleus, and *GAPDH* was used as a reference for high expression in the cytoplasm.

RNA fluorescence *in situ* hybridization

FISH was performed with the lncRNA FISH Kit (Guangzhou RiboBio, Guangzhou, China) according to the manufacturer's instructions. Briefly, cells were fixed with 4% formaldehyde for 10 min at room temperature. After being washed three times with PBS, cells were permeabilized with 0.5% Triton X-100 for 10 min at 4°C. Then, cells were incubated with RNA probes in hybridization buffer overnight at 37°C. The RNA probes were directly conjugated with a fluorophore. The cells were then washed three times with saline sodium citrate buffer and stained with DAPI. Images were captured by confocal microscopy (LSM700META; Zeiss, Oberkochen, Germany).

Mut seed sequences of miR-22-3p in the *Mir22hg*

WT and Mut seed sequences of miR-22-3p in the *Mir22hg* gene were ligated into pcDNA3.1. qRT-PCR analysis of miR-22-3p expression levels in C2C12 cells was performed 24 h after transfection with Mir22hg-mut and Mir22hg-WT overexpressing vectors in growth medium.

Target gene prediction and dual-luciferase reporter assays

Target genes were predicted using three bioinformatics software, miRTarBase (http://mirtarbase.cuhk.edu.cn/php/index.php), TargetScan (http://www.targetscan.org/mmu_72/), and RNA22 (https://cm.jefferson.edu/rna22).We used HEK293T cells to conduct the dual-luciferase reporter vector assays. HEK293T cells were cultured (8×10^4 cells/cm^2) in 12-well plates. When the cells reached 70%–80% confluence, 50 nM pmirGLO-HDAC4 luciferase vector (HDAC4-WT) or pmirGLO-*Mir22hg* Mut vector (HDAC4-Mut), in addition to 50 nM NC miR-22-3p mimic, was transfected with Lipofectamine 3000 Transfection Reagent (Invitrogen, Carlsbad, CA, USA) according to the manufacturer's instructions. After 24 h of transfection, the cells were harvested and luciferase assays were performed with the Dual-Luciferase Reporter Assay System (Promega, Madison, WI, USA) on a GloMax Luminometer (Promega, Madison, WI, USA) according to the manufacturer's instructions. For each sample, firefly luciferase activity was normalized , using *Renilla* luciferase activity to account for differences in transfection efficiency

Western blotting analysis

Cellular protein lysates in ice-cold radioimmunoprecipitation assay (RIPA) buffer (Beyotime, Shanghai, China) containing 1% phenylmethylsulfonyl fluoride (Beyotime) and 4% cOmplete Mini Protease Inhibitor Mixture (Roche, Mannheim, Germany) were collected after high-speed centrifugation (12,000 × *g*) for 10 min at 4°C. The protein concentration was detected with a BCA Protein Assay Kit (Beyotime). The protein extracts were added with 5× sodium dodecyl sulfate-polyacrylamide gel electrophoresis (SDS-PAGE) Sample Loading Buffer (Beyotime) and were denatured on a PCR instrument at 99.9°C for 10 min. Proteins were separated by SDS-PAGE, followed by transfer to polyvinylidene fluoride (PVDF) membranes (Millipore-Sigma, Billerica, MA, USA) for immunoblot assay. The primary antibodies used were as follows: MyHC (dilution 1:200; Developmental Studies Hybridoma Bank, Iowa City, IA, USA) and anti-MyoG (1:500, ABclonal, Wuhan, China), anti-HDAC4 and anti-MEF2C (dilution 1:500; ABclonal, Wuhan, China), and anti-α-Tubulin and anti-GAPDH

(dilution 1:2,000; Cell Signaling Technology, Danvers, MA, USA). Horseradish peroxidase-labeled anti-rabbit/goat IgG secondary antibody (dilution 1:5,000; Cell Signaling Technology) was used to detect protein expression. Targeted proteins were imaged on a Tanon 5200 instrument (Tanon, Shanghai, China) and analyzed with ImageJ software (National Institutes of Health, Bethesda, MD, USA). Western blot bands were quantified with ImageJ.[39]

Immunofluorescence staining

After transfection, C2C12 cells were cultured in a 12-well plate with differentiation medium (DM) for 3–4 days. The cells were then washed three times with PBS and fixed for 30 min in 4% paraformaldehyde, followed by three washes with PBS. The cells were subsequently incubated in ice-cold 0.5% Triton X-100 at 4°C for 15 min and washed a further three times. Next, the cells were incubated in blocking solution (1% bovine serum albumin) at room temperature (25°C) for 1 h. The cells were incubated with anti-MyHC antibody (dilution 1:50; Developmental Studies Hybridoma Bank) and anti-MyoG antibody (1:100; ABclonal, Wuhan, China) at 4°C for 16 h. The cells were then washed three times and incubated with Alexa Fluor 488-conjugated goat anti-mouse IgG (H+L) antibody (dilution 1:100; ZSGB-BIO, Beijing, China) and rhodamine [tetramethylrhodamine isothiocyanate (TRITC)]-conjugated goat anti-mouse IgG (H+L) antibody (dilution 1:100; ZSGB-BIO, Beijing, China) in the dark. After 1 h of incubation at room temperature, the cells were washed three times. The cell nuclei were stained with 4′,6-diamidino-2-phenylindole (DAPI) in the dark. After being washed three times, the glass slides were sealed with fluorescence anti-quenching agents (Biosharp, Hefei, China). Images were captured by confocal microscopy (LSM700META; Zeiss, Oberkochen, Germany). Quantification of immunofluorescence intensities was conducted with ImageJ.[40]

Lentiviral vector construction and lentivirus production

To generate *Mir22hg*-knockdown lentiviral vector, shRNA targeting *Mir22hg* or NC scramble sequences were subcloned into the GV112 vector (Shanghai GeneChem). The shRNA sequence (sh*Mir22hg*: 5¿-GGGATAGTACAATTGTGAA-3¿) was synthesized by Shanghai GeneChem. For production of the lentivirus, the expression vectors were co-transfected with packaging plasmid pHelper 1.0 vector (Shanghai GeneChem) and envelope plasmid pHelper 2.0 vector (Shanghai GeneChem) into HEK293T cells with the GeneChem transfection reagent (Shanghai GeneChem). The supernatant was collected 48 and 72 h after transfection, concentrated by ultracentrifugation at 25,000 rpm for 90 min, and resuspended in an appropriate volume of Opti-MEM. The lentivirus was concentrated by ultracentrifugation at 25,000 rpm for 90 min and stored at −80°C.

In vivo lentiviral particle administration

For the lentiviral particle administration experiment, we used sixty 8-week-old male mice. Mice were sacrificed by cervical dislocation, and all efforts were made to minimize animals' discomfort. Lentiviral particles for *Mir22hg* knockdown were injected into the mid-portion of one side of the TA muscles of each mouse at a dosage of 1.0×10^8 TU/mL. A total of 10 μL of viral preparation was injected into each muscle. Control lentivirus was injected into the left leg, and *Mir22hg*-knockdown lentivirus was injected into the right leg. At 2 days after lentiviral injection 1.2% $BaCl_2$ was injected, and the TA muscles were collected on days 0, 1, 3, 5, 7, 9, and 12 for H&E staining, qRT-PCR, and western blotting analysis. Moreover, the TA muscles collected at 12 days were weighed. H&E staining of TA muscles was performed according to a previous report.[41] The mean muscle fiber cross-sectional area was quantified with ImageJ Pro Plus according to a previous study protocol.[42,43] *Mir22hg* levels and mRNA levels of myogenic markers (*MyHC*, *α-Actin*) were detected by qRT-PCR. The protein levels of HDAC4 and myogenic markers (MyHC, MyoG) were evaluated by western blotting analysis.

Statistical analysis

Statistical analysis was performed with Prism 7 software (GraphPad Software, San Diego, CA, USA). Pearson correlation coefficients between the expression levels of *Mir22hg* and miR-22-3p and between the ratio of the weight of the right leg TA muscle of 28 adult male mice (8 weeks old) and the expression of *Mir22hg* in the TA muscle were calculated. A two-tailed Student's t test was used to analyze the statistical significance between two groups. Violin plots were drawn with R version 3.5.3. Data are expressed as mean values ± SEM unless otherwise noted, and the level of significance was set at $p < 0.05$.

SUPPLEMENTAL INFORMATION

Supplemental Information can be found online at https://doi.org/10.1016/j.omtn.2021.02.025.

ACKNOWLEDGMENTS

This work was supported by the National Science and Technology Major Project (2016ZX08006001-003) and the Major Agricultural Plan of New Variety Innovation of Jiangsu Province (PZCZ201734).

AUTHOR CONTRIBUTIONS

H.L., W.W., and R.L. conceived and designed the experiments; R.L. performed the experiments; Y.C., W.L., W.D., L.Z., X.Z., C.N., H.L., C.J., and J.T. contributed reagents and materials; R.L., B.L., and Y.Y. analyzed the data. R.L. and W.W. drafted the manuscript, and W.W. and H.L. revised the manuscript.

DECLARATION OF INTERESTS

The authors declare no competing interest.

REFERENCES

1. Muñoz-Cánoves, P., Carvajal, J.J., Lopez de Munain, A., and Izeta, A. (2016). Editorial: Role of Stem Cells in Skeletal Muscle Development, Regeneration, Repair, Aging, and Disease. Front. Aging Neurosci. *8*, 95.

2. Atianand, M.K., Caffrey, D.R., and Fitzgerald, K.A. (2017). Immunobiology of Long Noncoding RNAs. Annu. Rev. Immunol. *35*, 177–198.

3. Flynn, R.A., and Chang, H.Y. (2014). Long noncoding RNAs in cell-fate programming and reprogramming. Cell Stem Cell *14*, 752–761.

4. Fatica, A., and Bozzoni, I. (2014). Long non-coding RNAs: new players in cell differentiation and development. Nat. Rev. Genet. *15*, 7–21.

5. Choudhari, R., Sedano, M.J., Harrison, A.L., Subramani, R., Lin, K.Y., Ramos, E.I., Lakshmanaswamy, R., and Gadad, S.S. (2020). Long noncoding RNAs in cancer: From discovery to therapeutic targets. Adv. Clin. Chem. *95*, 105–147.

6. Yao, R.W., Wang, Y., and Chen, L.L. (2019). Cellular functions of long noncoding RNAs. Nat. Cell Biol. *21*, 542–551.

7. Wang, S., Jin, J., Xu, Z., and Zuo, B. (2019). Functions and Regulatory Mechanisms of lncRNAs in Skeletal Myogenesis, Muscle Disease and Meat Production. Cells *8*, 1107.

8. Sweta, S., Dudnakova, T., Sudheer, S., Baker, A.H., and Bhushan, R. (2019). Importance of Long Non-coding RNAs in the Development and Disease of Skeletal Muscle and Cardiovascular Lineages. Front. Cell Dev. Biol. *7*, 228.

9. Zhao, Y., Chen, M., Lian, D., Li, Y., Li, Y., Wang, J., Deng, S., Yu, K., and Lian, Z. (2019). Non-Coding RNA Regulates the Myogenesis of Skeletal Muscle Satellite Cells, Injury Repair and Diseases. Cells *8*, 988.

10. Cesana, M., Cacchiarelli, D., Legnini, I., Santini, T., Sthandier, O., Chinappi, M., Tramontano, A., and Bozzoni, I. (2011). A long noncoding RNA controls muscle differentiation by functioning as a competing endogenous RNA. Cell *147*, 358–369.

11. Zhu, M., Liu, J., Xiao, J., Yang, L., Cai, M., Shen, H., Chen, X., Ma, Y., Hu, S., Wang, Z., et al. (2017). Lnc-mg is a long non-coding RNA that promotes myogenesis. Nat. Commun. *8*, 14718.

12. Yu, X., Zhang, Y., Li, T., Ma, Z., Jia, H., Chen, Q., Zhao, Y., Zhai, L., Zhong, R., Li, C., et al. (2017). Long non-coding RNA Linc-RAM enhances myogenic differentiation by interacting with MyoD. Nat. Commun. *8*, 14016.

13. Anderson, D.M., Anderson, K.M., Chang, C.L., Makarewich, C.A., Nelson, B.R., McAnally, J.R., Kasaragod, P., Shelton, J.M., Liou, J., Bassel-Duby, R., and Olson, E.N. (2015). A micropeptide encoded by a putative long noncoding RNA regulates muscle performance. Cell *160*, 595–606.

14. Li, Y., Yuan, J., Chen, F., Zhang, S., Zhao, Y., Chen, X., Lu, L., Zhou, L., Chu, C.Y., Sun, H., and Wang, H. (2020). Long noncoding RNA SAM promotes myoblast proliferation through stabilizing Sugt1 and facilitating kinetochore assembly. Nat. Commun. *11*, 2725.

15. Yang, C.P., Yang, W.S., Wong, Y.H., Wang, K.H., Teng, Y.C., Chang, M.H., Liao, K.H., Nian, F.S., Chao, C.C., Tsai, J.W., et al. (2020). Muscle atrophy-related myotube-derived exosomal microRNA in neuronal dysfunction: Targeting both coding and long noncoding RNAs. Aging Cell *19*, e13107.

16. McMullen, J.R., and Drew, B.G. (2016). Long non-coding RNAs (lncRNAs) in skeletal and cardiac muscle: potential therapeutic and diagnostic targets? Clin. Sci. (Lond.) *130*, 2245–2256.

17. Dey, B.K., Pfeifer, K., and Dutta, A. (2014). The H19 long noncoding RNA gives rise to microRNAs miR-675-3p and miR-675-5p to promote skeletal muscle differentiation and regeneration. Genes Dev. *28*, 491–501.

18. Chen, R., Jiang, T., She, Y., Xie, S., Zhou, S., Li, C., Ou, J., and Liu, Y. (2018). Comprehensive analysis of lncRNAs and mRNAs with associated co-expression and ceRNA networks in C2C12 myoblasts and myotubes. Gene *647*, 164–173.

19. Zhou, J., Zhang, S., Wang, H., and Sun, H. (2017). LncFunNet: an integrated computational framework for identification of functional long noncoding RNAs in mouse skeletal muscle cells. Nucleic Acids Res. *45*, e108.

20. Wei, X., Li, H., Zhang, B., Li, C., Dong, D., Lan, X., Huang, Y., Bai, Y., Lin, F., Zhao, X., and Chen, H. (2016). miR-378a-3p promotes differentiation and inhibits proliferation of myoblasts by targeting HDAC4 in skeletal muscle development. RNA Biol. *13*, 1300–1309.

21. Zetser, A., Gredinger, E., and Bengal, E. (1999). p38 mitogen-activated protein kinase pathway promotes skeletal muscle differentiation. Participation of the Mef2c transcription factor. J. Biol. Chem. *274*, 5193–5200.

22. Dumont, N.A., Bentzinger, C.F., Sincennes, M.C., and Rudnicki, M.A. (2015). Satellite Cells and Skeletal Muscle Regeneration. Compr. Physiol. *5*, 1027–1059.

23. Hezroni, H., Koppstein, D., Schwartz, M.G., Avrutin, A., Bartel, D.P., and Ulitsky, I. (2015). Principles of long noncoding RNA evolution derived from direct comparison of transcriptomes in 17 species. Cell Rep. *11*, 1110–1122.

24. Cabili, M.N., Dunagin, M.C., McClanahan, P.D., Biaesch, A., Padovan-Merhar, O., Regev, A., Rinn, J.L., and Raj, A. (2015). Localization and abundance analysis of human lncRNAs at single-cell and single-molecule resolution. Genome Biol. *16*, 20.

25. Jin, J.J., Lv, W., Xia, P., Xu, Z.Y., Zheng, A.D., Wang, X.J., Wang, S.S., Zeng, R., Luo, H.M., Li, G.L., and Zuo, B. (2018). Long noncoding RNA *SYISL* regulates myogenesis by interacting with polycomb repressive complex 2. Proc. Natl. Acad. Sci. USA *115*, E9802–E9811.

26. Wang, D.Z., Valdez, M.R., McAnally, J., Richardson, J., and Olson, E.N. (2001). The Mef2c gene is a direct transcriptional target of myogenic bHLH and MEF2 proteins during skeletal muscle development. Development *128*, 4623–4633.

27. Li, Z., Cai, B., Abdalla, B.A., Zhu, X., Zheng, M., Han, P., Nie, Q., and Zhang, X. (2019). LncIRS1 controls muscle atrophy via sponging miR-15 family to activate IGF1-PI3K/AKT pathway. J. Cachexia Sarcopenia Muscle *10*, 391–410.

28. Zhou, L., Sun, K., Zhao, Y., Zhang, S., Wang, X., Li, Y., Lu, L., Chen, X., Chen, F., Bao, X., et al. (2015). Linc-YY1 promotes myogenic differentiation and muscle regeneration through an interaction with the transcription factor YY1. Nat. Commun. *6*, 10026.

29. Luo, L., Martin, S.C., Parkington, J., Cadena, S.M., Zhu, J., Ibebunjo, C., Summermatter, S., Londraville, N., Patora-Komisarska, K., Widler, L., et al. (2019). HDAC4 Controls Muscle Homeostasis through Deacetylation of Myosin Heavy Chain, PGC-1α, and Hsc70. Cell Rep. *29*, 749–763.e12.

30. Choi, M.C., Ryu, S., Hao, R., Wang, B., Kapur, M., Fan, C.M., and Yao, T.P. (2014). HDAC4 promotes Pax7-dependent satellite cell activation and muscle regeneration. EMBO Rep. *15*, 1175–1183.

31. Wu, X., Li, H., Park, E.J., and Chen, J.D. (2001). SMRTE inhibits MEF2C transcriptional activation by targeting HDAC4 and 5 to nuclear domains. J. Biol. Chem. *276*, 24177–24185.

32. Lv, W., Jin, J., Xu, Z., Luo, H., Guo, Y., Wang, X., Wang, S., Zhang, J., Zuo, H., Bai, W., et al. (2020). lncMGPF is a novel positive regulator of muscle growth and regeneration. J. Cachexia Sarcopenia Muscle *11*, 1723–1746.

33. Zhang, Z.K., Li, J., Guan, D., Liang, C., Zhuo, Z., Liu, J., Lu, A., Zhang, G., and Zhang, B.T. (2018). A newly identified lncRNA MAR1 acts as a miR-487b sponge to promote skeletal muscle differentiation and regeneration. J. Cachexia Sarcopenia Muscle *9*, 613–626.

34. Lin, Q., Schwarz, J., Bucana, C., and Olson, E.N. (1997). Control of mouse cardiac morphogenesis and myogenesis by transcription factor MEF2C. Science *276*, 1404–1407.

35. Potthoff, M.J., Arnold, M.A., McAnally, J., Richardson, J.A., Bassel-Duby, R., and Olson, E.N. (2007). Regulation of skeletal muscle sarcomere integrity and postnatal muscle function by Mef2c. Mol. Cell. Biol. *27*, 8143–8151.

36. Livak, K.J., and Schmittgen, T.D. (2001). Analysis of relative gene expression data using real-time quantitative PCR and the 2(-Delta C(T)) Method. Methods *25*, 402–408.

37. Li, R., Li, B., Shen, M., Cao, Y., Zhang, X., Li, W., Tao, J., Wu, W., and Liu, H. (2020). LncRNA 2310043L19Rik inhibits differentiation and promotes proliferation of myoblast by sponging miR-125a-5p. Aging (Albany NY) *12*, 5625–5639.

38. Chen, X., He, L., Zhao, Y., Li, Y., Zhang, S., Sun, K., So, K., Chen, F., Zhou, L., Lu, L., et al. (2017). *Malat1* regulates myogenic differentiation and muscle regeneration through modulating MyoD transcriptional activity. Cell Discov. *3*, 17002.

39. Concepcion, C.P., Han, Y.C., Mu, P., Bonetti, C., Yao, E., D'Andrea, A., Vidigal, J.A., Maughan, W.P., Ogrodowski, P., and Ventura, A. (2012). Intact p53-dependent responses in miR-34-deficient mice. PLoS Genet. *8*, e1002797.

40. Dudley, L.J., Cabodevilla, A.G., Makar, A.N., Sztacho, M., Michelberger, T., Marsh, J.A., Houston, D.R., Martens, S., Jiang, X., and Gammoh, N. (2019). Intrinsic lipid binding activity of ATG16L1 supports efficient membrane anchoring and autophagy. EMBO J. *38*, e100554.

41. Zhang, L., Zhang, S., Song, H., and Li, B. (2018). Effect of Collagen Hydrolysates from Silver Carp Skin (*Hypophthalmichthys molitrix*) on Osteoporosis in Chronologically Aged Mice: Increasing Bone Remodeling. Nutrients *10*, 1434.

42. Guo, S.L., Tan, G.H., Li, S., Cheng, X.W., Zhou, Y., Jia, Y.F., Xiong, H., Tao, J., and Xiong, Z.Q. (2012). Serum inducible kinase is a positive regulator of cortical dendrite development and is required for BDNF-promoted dendritic arborization. Cell Res. *22*, 387–398.

43. Zhang, S.M., Zhu, L.H., Chen, H.Z., Zhang, R., Zhang, P., Jiang, D.S., Gao, L., Tian, S., Wang, L., Zhang, Y., et al. (2014). Interferon regulatory factor 9 is critical for neointima formation following vascular injury. Nat. Commun. *5*, 5160.